

Soft Matter

Accepted Manuscript



This is an *Accepted Manuscript*, which has been through the Royal Society of Chemistry peer review process and has been accepted for publication.

Accepted Manuscripts are published online shortly after acceptance, before technical editing, formatting and proof reading. Using this free service, authors can make their results available to the community, in citable form, before we publish the edited article. We will replace this *Accepted Manuscript* with the edited and formatted *Advance Article* as soon as it is available.

You can find more information about *Accepted Manuscripts* in the [Information for Authors](#).

Please note that technical editing may introduce minor changes to the text and/or graphics, which may alter content. The journal's standard [Terms & Conditions](#) and the [Ethical guidelines](#) still apply. In no event shall the Royal Society of Chemistry be held responsible for any errors or omissions in this *Accepted Manuscript* or any consequences arising from the use of any information it contains.



Journal Name

ARTICLE

Competitive adsorption of amylopectin and amylose on cationic nanoparticles: study on the aggregation mechanism

Frida Iselau,^{a,b} Tuan Phan Xuan,^c Aleksandar Matic,^c Michael Persson,^d Krister Holmberg,^a and Romain Bordes^{a,e}

Received 00th January 20xx,
Accepted 00th January 20xx

DOI: 10.1039/x0xx00000x

www.rsc.org/

In this study we investigate the interactions between cationic nanoparticles and anionic starch, where the starch was composed of 20 wt% of amylose, a linear polymer, and 80 wt% of amylopectin, a branched polymer. The mechanism of aggregation was investigated by scattering techniques. It was found that the cationic particles formed large aggregates with the starch as a result of selective adsorption of the amylopectin. Amylose did not participate significantly in the aggregate formation even when the charge ratio of starch to particles was <1. For starch to particles ratio >1 stabilization was recovered mostly due to the large hindrance brought about by the highly branched amylopectin. This results in a shift of stabilization mechanism from electrostatic to electrosteric. The internal structure of the aggregates was composed of primary particles with starch coils adsorbed on the surface. This information supports the proposed aggregation mechanism, which is based on adsorption of the negatively charged starch in patches on the positively charged nanoparticles causing attractive interaction between the particles.

Introduction

The combination of polyelectrolytes (PEs) with charged colloids is a topic of high relevance for many industrial applications. The need for understanding the interaction between PEs and colloidal particles has generated a large number of studies focusing on the behaviour of the particles in presence of PEs and on understanding how the adsorption of PEs at the surface of the particles can influence the behaviour of the colloidal suspension.^{1–5} The adsorption of PEs at colloidal particle surfaces carrying an opposite charge has been investigated for many types of systems. The colloidal particle has typically been a latex or silica nanoparticles and the PE has been DNA, polyacrylamide, polystyrene sulfonate, polyvinyl amine, polyacrylic acid, and many more. Anionic nanoparticles combined with a cationic polymer has been a particularly popular combination,^{2, 4, 6–8} owing to the natural abundance of negatively charged colloids.¹

When a polyelectrolyte is added to a suspension of oppositely charged particles it adsorbs at the particle surface, mostly due to electrostatic attraction. This adsorption reduces the entropy of the polymer, which is energetically unfavourable, but the adsorption can be seen as an ion exchange process in which the large polyelectrolyte replaces

small inorganic ions as counterions around the surface. There is a strong entropy gain in this type of ion exchange and the overall result is that the system's entropy is increased.^{9–11} Unlike the situation with simple salts, where the aggregation of charged particles is caused by screening of the repulsive forces between the particles when the ionic strength increases, and where further salt addition will not restore stability, the aggregation of charged particles by the adsorption of an oppositely charged PE can be reversible,⁷ since the colloidal behaviour depends strongly on the PE concentration. At low PE concentration, the surface charge first decreases. Under these conditions, aggregation occurs through bridge or patchwise flocculation. Further addition of PE can cause reversal of the surface charge. The polymer adsorption on the particle surface is then driven by non-electrostatic attractive interactions,¹² such as van der Waals interactions, eventually leading to an overload of PE on the particle surface. This charge reversal may, under certain conditions, lead to restabilization of the PE-particle complexes. In most of the systems previously studied, involving cationic particles and anionic PE, as well as the reverse, the focus has been on how the nature of the PE (molecular weight and charge density), the pH and the ionic strength affect the aggregation behaviour.

There is a plethora of important applications of PE-particle interactions, ranging from consumer products such as pharmaceuticals, food and personal care formulations to industrial processes such as coatings, water treatment, mineral ore processing and papermaking. The stability of the suspension, the rheology and the adhesion properties are often tuned by the PE-particle interaction.^{13–16} This type of interaction is particularly important in the paper making process. Combinations of negatively charged nanoparticles and cationic PEs are commonly used for flocculation, retention

^a Department of Chemistry and Chemical Engineering, Chalmers University of Technology, 412 96 Göteborg, Sweden. E-mail: frida.iselau@chalmers.se

^b Kemira Kemi AB, 442 40 Kungälv, Sweden

^c Department of Applied Physics, Chalmers University of Technology, 412 96 Göteborg, Sweden

^d AkzoNobel Pulp and Performance Chemicals AB, 445 80 Bohus, Sweden

^e Vinn Excellence Center SuMo Biomaterials, Chalmers University of Technology, 412 96 Gothenburg, Sweden. E-mail: bordes@chalmers.se

enhancement and strengthening purposes.¹⁷⁻¹⁹ Latex/PE systems are used for surface hydrophobation of paper, referred to as surface sizing. In the latter process starch is commonly used in combination with positively or negatively charged latexes. The starch and the latex are usually premixed and then applied on the paper surface in the dry-end of the paper machine.^{20, 21} Typical concentrations are around a few percent starch and around 0.1 % particles.

In this work we have studied the aggregate formation mechanism for the system anionic starch-positively charged particles by investigating the aggregation behaviour against PE concentration and the internal structure of the formed aggregates. The aggregation formation path has been investigated by variation of the order of addition. The effect of particle concentration has been evaluated and the impact of the starch composition has been demonstrated by comparing results from regular starch with those from waxy starch.

We have used different scattering techniques; dynamic light scattering (DLS), static light scattering (SLS) and small angle light scattering (SAXS) to study the aggregation process in the presence of starch for different length scales.

Experimental section

Materials

The starch powders, oxidized regular potato starch and oxidized waxy potato starch, were both from Avebe, The Netherlands, and used as received. The cationic particles, denoted SP+, were synthesized as described in a previous paper.²¹ Milli-Q water (resistivity > 18 M Ω) was used for the preparation of the aqueous solutions.

Methods

Starch cooking

3.5 g of starch powder was suspended in 100 ml Milli-Q water under stirring. The suspension was boiled for 10 minutes rendering a clear, slightly pale yellow starch solution. The cooled starch solution was diluted to a final concentration of 3 wt% calculated on dry weight of the starch.

Particle size determination by light scattering

A multi angle light scattering instrument ALV/CGS-8F was used in order to perform dynamic and static light scattering measurement on the SP+ particles and on the particle-starch aggregates. The instrument was equipped with a laser source of 150 mW and a wavelength $\lambda = 532$ nm. The temperature was controlled by a thermostat bath to within ± 0.2 °C. Measurements were made at angles of observation (θ) between 12 and 155 degrees. For the particle size measurement of the cationic particle suspension a sample was prepared by diluting the particle suspension in Milli-Q to a concentration of 0.05 wt%. The sample was filtered with a 0.2 μ m hydrophilic syringe filter (Sartorius) before measurement. For the particle size measurements of the cationic particle suspension in combination with the anionic starch the SP+ concentration was 0.1 wt%. The 3 wt% starch solution was added in different amounts to the particle suspension. Both SP+ and the starch were filtered with 0.2 μ m hydrophilic syringe filter (Sartorius) before mixing. After 5 min waiting time the samples were measured.

Static light scattering, SLS

The relative scattering intensity (I_r) was calculated as the intensity minus the solvent scattering divided by the scattering intensity of toluene at 20 °C. In dilute solutions I_r is related to the weight average molar mass (M_w) and the structure factor ($S(q)$) of the solute.²²

In this study, a Rayleigh constant of $1.35 \times 10^{-5} \text{ cm}^{-1}$ for toluene was used. The z-average radius of gyration (R_{Gz}) was determined from the initial q-dependence of $S(q)$.

The dn/dc for SP+ was experimentally determined to 0.0209 mL/g.

Dynamic light scattering, DLS

The intensity autocorrelation function measured with DLS is related to the normalized electric field correlation function, $g_1(t)$, by the Siegert relation.²² $g_1(t)$ was analyzed in terms of a distribution of relaxation time, since in dilute solutions the relaxation is caused by self-diffusion of the particles. The hydrodynamic radius (R_H) was calculated from the diffusion coefficient using the Stokes-Einstein equation. The z-average hydrodynamic radius (R_{Hz}) was determined from the average diffusion coefficient.

ζ potential

The ζ potential was measured using a Malvern Nano instrument and disposable measuring cells. ζ potential was calculated using the in-build software that employs similar models as for phase analysis light scattering.²³ For the ζ potential measurements on the cationic particle suspension, a sample was prepared by diluting the particle suspension to a concentration of 0.05 wt%. The sample was filtered with 0.2 μ m hydrophilic syringe filter (Sartorius) before measurement. For the ζ potential measurements on the cationic particle suspension in combination with the anionic starch the SP+ concentration was 0.1 wt% and a 3 wt% starch solution was added in different amounts to the particle suspension. Both the SP+ and the starch were filtered with 0.2 μ m hydrophilic syringe filter (Sartorius) before mixing. The samples were analyzed 5 min after the starch addition and no background electrolyte was used. pH remained constant throughout the titration around 4.0.

Particle charge density titration

Particle charge density titration was performed using a Particle Charge Detector, CAS Charge Analyzing System (AFG, Analytic GMBH). The method is an electrokinetic technique where the charge distribution is determined by measuring the streaming potential.^{24, 25} The sample was titrated with a titrant carrying the opposite charge and the amount of titrant required for charge neutralization at a macroscopic level, is used for calculating the charge ratio. The samples were filtered with 0.2 μ m hydrophilic syringe filter (Sartorius) before measurement. A charge titration of the cationic particles with the anionic starch as the titrant was performed in order to investigate the particle to starch ratio at charge neutralization.

Turbidity

The turbidity measurements were performed on an Agilent Cary 60 UV/Vis instrument using a quartz cuvette. The baseline was recorded in Milli-Q water. The value of the absorbance at

400 nm was used as a measure of the turbidity. The particle suspension, 0.1 wt%, was filtered with 0.2 μm hydrophilic syringe filter (Sartorius) before 2 mL sample was transferred to the cuvette. The starch solution was also filtered with 0.2 μm hydrophilic syringe filter (Sartorius) before titration. The titrations were carried out as follows. To 2 mL sample in a cuvette 20 μL aliquots of a 3 wt% starch solution were successively added.

In addition, titrations were also performed during stirring. A beaker with 20 mL of filtered sample of 0.1 wt% particle suspension was put on a magnetic stirrer plate. 500 μL aliquots of a 3 wt% starch solution were successively added to the vortex of the particle suspension. After a mixing time of 30 seconds a 2 mL sample was taken from the mixture and transferred to the cuvette for UV/Vis measurement. After the measurement the 2 mL sample was returned to the beaker and a new addition of starch was done.

To examine the effect of the titration, where the starch was successively added in small aliquots, another series was performed where the starch was added in larger amounts to individual particle samples, i.e. to 2 mL samples of SP+, 0.1 wt%, was added 50, 100, 150, 200, 300, 400 or 500 μL of the 3 wt% starch solution.

Finally the importance of the order of addition was assessed. To 1 mL starch with increasing concentrations 1 mL of 0.2 wt% particle suspension was added yielding a final concentration of 0.1 wt% particles. To be able to compare with the results where starch was added to the 2 mL particle suspension water was added to reach the same dilution.

Small angle X-Ray scattering, SAXS

Small angle X-ray scattering (SAXS) experiments were carried out at the I911-4 beamline of the MAX-Lab laboratory synchrotron using a wavelength of 0.91 \AA . The samples were analyzed in capillaries maintained at 20 $^{\circ}\text{C}$ and were prepared 24 h prior to the measurements. The SP+ and starch mixtures were prepared by adding different amounts of the 3 wt% starch solution to samples of 2 mL of a 0.1 wt% SP+ suspension. The particle suspension and the starch solution were filtered with 0.2 μm hydrophilic syringe filter (Sartorius) before addition.

For each sample, the scattering of pure solvent (Milli-Q water) was also measured. Two-dimensional SAXS images were recorded using a PILATUS 1 M detector (Dectris) with an exposure time of 120 s. The scattering vector q ($q = 4\pi \sin \theta / \lambda$, where λ is the wavelength and 2θ is the scattering angle) was calibrated with a silver behenate sample. Reported scattering profiles $I(q)$ were obtained as the difference of the radial averaged SAXS 2D images from the sample and solvent. Data reduction was processed using Nika package on Igor pro.²⁶

SEC-MALS/RI

A Size Exclusion Chromatography system with Multiple Angle Light Scattering and Refractive Index (SEC-MALS/RI) detector from Wyatt Technology was used to analyze the concentration and molecular weight distribution for starch in solution. The RI detector was an Optilab T-rEX and the MALS detector was a Dawn Heleos-II. Injections were done with a Waters 717plus Autosampler and an in-line degasser from Waters for degassing the mobile phase was used. The separation column was a TSKgel GMPWXL with the dimensions of 7.8 mm x 30.0 cm and with a particle size of 13.0 μm from Tosch Bioscience. The mobile phase was

10 mM NaCl+0.02 wt% NaN_3 and it was filtered and degassed before used in the SEC system. The flow rate was 0.5 ml/min and the elution time was 30 min. In the sequence, the mobile phase was used as blank and a Pullulan standard was used for quality control. Triple injections of the samples were done.

The samples for the SEC analysis were prepared as follows. A 3 wt% starch solution was cooked as described above. The starch and the 0.1 wt% SP+ suspension were filtered with 0.2 μm hydrophilic syringe filter (Sartorius) before mixing. The samples were prepared by adding starch in different amounts to a 10 mL SP+, 0.1 wt% sample. After the starch addition the samples were shaken and thereafter let to equilibrate for at least 15 min. For centrifugation 6 g of each sample was transferred to tubes and put in the centrifuge (Universal 32 from Hettich); 9000 rpm for 2x10 min. After the centrifugation of the SP+ and starch mixtures the supernatant was removed and filtered through a 0.1 μm filter (PALL Acrodisc). To verify that the starch in solution was not affected by the centrifugation or the filtration step, a starch sample diluted with Milli-Q was prepared and treated the same way as the particles+starch samples. The filtrates were then injected in the SEC-MALS/RI after dilution 1:1 with Milli-Q water. Also included in the SEC analysis was a starch sample diluted with Milli-Q without any further treatment to be used as reference. The dn/dc value was set to 0.151 mL/g according to literature.²⁷

Results and discussion

Description of the system studied

Starch is a biopolymer with glucose as the repeating unit connected through α (1 \rightarrow 4)-glycosidic bonds. The polyanhydroglucose chain can form two types of polymers: amylose and amylopectin. The amylose chains are linear and relatively short while the amylopectin is highly branched and of high molecular weight. Different types of native starch have different proportions of amylopectin and amylose in the granules. The composition of regular potato starch is typically 20 wt% amylose and 80 wt% amylopectin.²⁸ In contrast, a waxy starch contains only amylopectin. Native starch has a very high average molecular weight and gives rise to very high viscosity when dissolved in water. Therefore the starch is often oxidized in order to decrease the molecular weight, which leads to reduced solution viscosity. This oxidation is typically done with sodium hypochlorite (NaClO). The starch granules are first dispersed in a sodium hydroxide solution at pH 9.5 and NaClO is then added. The process leads to depolymerization of the starch and at the same time oxidation of hydroxyl groups on the anhydroglucose rings to carboxylic groups.²⁹ Thus, oxidized starch will have lower molecular weight and carry an anionic charge, which will be pH dependent. The charge density depends on the amount of NaClO added, and typical values of degree of substitution (carboxyl groups) are 0.03-0.05 for oxidized potato starch. For the regular starch used in this work the weight average molecular weight (M_w) was determined to 870 kDa with a M_w/M_n of 4.3. Radius of gyration (R_g) was 7 nm. The M_w for the waxy starch was determined to 3090 kDa and the M_w/M_n was 2.3. The higher M_w/M_n ratio for the regular starch is due to the presence of short chained amylose molecules. R_g was also measured to be 7 nm.

The cationic particles, SP+, used in this study consist of a hydrophobic core of styrene-acrylate copolymer. Colloidal stability is achieved by a cationic stabilizer. The cationic stabilizer is a copolymer of styrene and quaternary ammonium monomers.²¹ SP+ has a hydrodynamic radius of 22 nm and a R_G of 14 nm, with a ζ potential of +53 mV. Starch has very low scattering intensity; therefore values of ζ potential could not be obtained.

Using a particle charge detector, PCD, the charge ratio between starch and particles was determined. The anionic starch was used as the titrant for the cationic particles in order to examine the amount of starch needed for charge neutralization of the particles. The anionic demand for 1 mg of SP+ particles was 2.1 mg starch, i.e. a 1:2.1 mass ratio was needed to obtain 1:1 in charge ratio. The amount of starch added to the particle suspensions in this study was converted to actual charge ratio using this relation and the charge ratio will in the following be used for describing the relation between the particles and the starch.

Aggregate formation

Formation of aggregates at different PE concentrations was monitored by measuring the turbidity of a 0.1 wt% particle suspension with an UV-visible spectrophotometer at 400 nm. The titrations were carried out by adding small fractions of anionic starch to the dispersion using an equilibration time of 5 minutes.

Figure 1 shows the turbidity of the suspension of SP+ plotted against starch addition. First, the addition of starch induced a dramatic increase in turbidity due to formation of aggregates in the system. The aggregation took place even at very low starch to particle ratio, showing that the stability of the cationic particle suspension was strongly affected by the oppositely charged polyelectrolyte. The turbidity increased further with increasing addition of starch. This is in accordance with previous studies of similar systems.^{2, 3, 7, 8, 30} The turbidity increased to a maximum at a starch to particle charge ratio of 1.1:1. Further addition of starch partially restored the stability of the dispersion, as is evident from the decrease in turbidity above this charge ratio. However, the turbidity did not return to the initial value for the bare cationic particles, indicating that even under the presence of an excess of starch, there are still aggregates in the suspension.

The aggregation behaviour was further investigated by using different particle concentrations, different ways of mixing and different addition orders. The stirring rate^{31, 32} and the addition order^{6, 33, 34} have in previous studies been found to have a crucial impact on the aggregate formation.

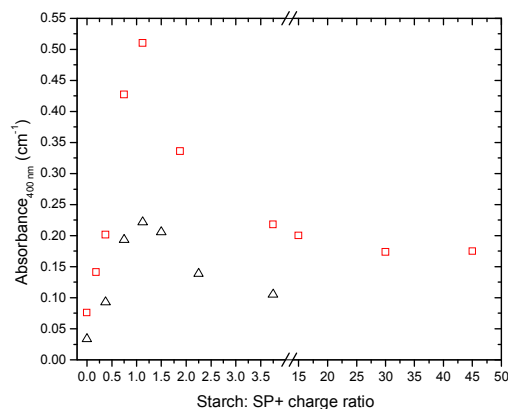


Fig. 1 Turbidity of the cationic particle (SP+) suspension vs. starch to SP+ charge ratio. Two different particle concentrations were used; 0.1 wt% (squares), 0.05 wt% (triangles). Note the break in the x axis.

Most of the work was performed with a SP+ concentration of 0.1 wt%. To verify that aggregation occurs also at higher and lower SP+ concentrations, titrations were performed with SP+ concentrations of 0.05 wt%, 0.2 wt% and 0.5 wt%. It was found that the aggregation behaviour was very similar for all the particle concentrations. This is illustrated in Figure 1, which shows titration curves for SP+ and starch using a particle concentration of either 0.1 wt% or 0.05 wt%. The turbidity profiles were the same and it is only the intensity of the turbidity that was affected by the initial particle concentration. The radius of the formed aggregates at the particle concentrations 0.05 wt% and 0.1 wt% was similar, 65 nm and 56 nm, respectively. Thus, the aggregate size was not concentration dependent within the range used in this study.

Different ways of addition were also investigated. The reference method consists of adding starch to the particle suspension in a cuvette, hand shaking and then measuring after 5 minutes. Addition of the starch to the particle suspension during intensive stirring was also tested and gave the same turbidity curve as the reference method. The mixing rate and mixing time have previously been reported to have an impact on formation of polyelectrolyte complexes,^{31, 32, 35} but for the system studied here with small cationic nanoparticles and an anionic polymer of relatively high molecular weight the stirring rate seemed to have no effect on the size of the formed aggregates.

The order of addition, i.e. adding the polyelectrolyte to the particle suspension or vice versa, has been reported to have an impact on the aggregation behaviour.^{6, 33-35} The two modes of addition were tested and the results are shown in Figure 2. The figure shows that the aggregation behaviour, as manifested by a turbidity increase, was the same.

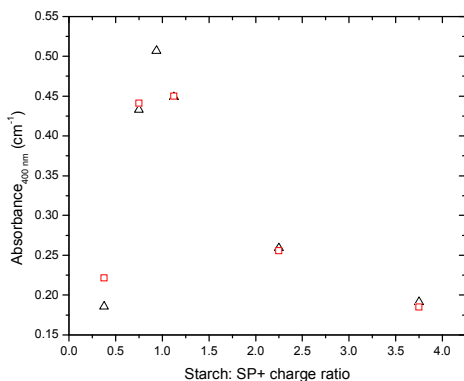


Fig. 2 Turbidity curves for different orders of addition, starch to particles and particles to starch. Starch solution added to SP+ suspension (squares) and SP+ suspension added to starch solution (triangles).

The long term stability of the suspension of aggregates was evaluated by measuring the turbidity after storing the samples for two weeks at room temperature. It was found that the turbidity values were the same as before storage. Thus, the aggregate suspension seemed to have reasonable storage stability.

Aggregate characterization

The formed aggregates were investigated further by dynamic light scattering and ζ potential measurements. Different particle to starch ratios were analyzed by adding varying amounts of a 3 wt% starch solution to 2 mL of the 0.1 wt% particle suspension. The results with respect to ζ potential, hydrodynamic radius and turbidity as function of the starch to particle charge ratio, are shown in Figure 3. As can be seen, the size, as determined with DLS, followed rather well the turbidity curve at low starch to particle ratios. Both curves exhibited a maximum at a charge ratio of around 1. Beyond the maximum the particle size curve deviated from the turbidity curve, however. Whereas the hydrodynamic radius levelled out around 45 nm, the absorbance decreased continuously. The reason for this apparent discrepancy will be discussed below. DLS measurements were also carried out on pure starch. However, these experiments did not give satisfactory scattering signals, which mean that there was no information about the starch size. Furthermore, it was found that starch only, at the relevant concentration, influenced the viscosity of the formulation to a negligible extent.

The ζ potential is a measure of the neutralization of the positive charge of the particles through adsorption of the anionic starch, a process that will lead to loss of electrostatic stabilization. When anionic starch was successively added to the cationic particle suspension the ζ potential decreased and reached zero at the same starch to particle charge ratio as gave the optimum in turbidity and particle size. The ζ potential then levelled out at around -8 mV. This is a low negative charge and it is unlikely that electrostatic interactions only could provide proper stability of the aggregates.³⁶ It is likely that the branched starch molecules provide an additional steric component to the stabilization of the colloidal system.

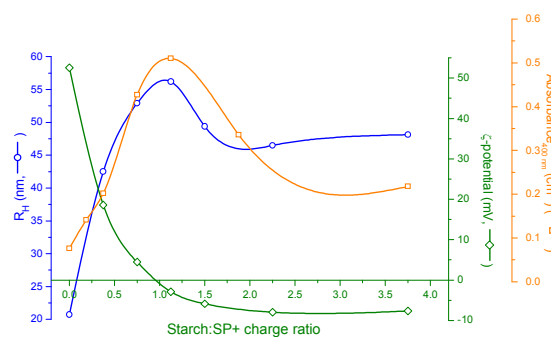


Fig. 3 Plot of hydrodynamic radius (circles) and zeta potential (triangles) (left y-axis) and turbidity (squares) (right y-axis) vs. starch to particle charge ratio.

According to Figure 3 maximum turbidity, maximum particle size and the cross-over from positive to negative ζ potential all occur at a starch to particle charge ratio of 1:1 or slightly above, i.e. close to unity.

Several authors have demonstrated that on addition of a polyelectrolyte to a suspension of oppositely charged colloidal particles there is a minimum in stability at a certain amount of added polyelectrolyte.^{2, 8, 30, 37, 38} This is in accordance with the turbidity results in this study, the maximum in turbidity corresponding to the most destabilized particle system.

The study of the size of the aggregates by DLS was complemented by static light scattering (SLS) measurements at different starch to particle ratios. The measurements were performed on diluted systems where the size determination is independent of the concentration. The R_G for the bare particles was obtained from SAXS since the SLS data were not satisfactory. Figure 4 shows the change in the ratio between radius of gyration (R_G), obtained from SAXS or SLS, and radius of hydration (R_H) determined by DLS when the starch to particle ratio was varied.

The value before starch addition corresponds well to what is expected for particles stabilized by a layer of polymer as used in the present work.³⁹ On addition of starch, the R_G/R_H ratio first reached a plateau value at around 1. At a starch to particles charge ratio of around 1, i.e. the ratio corresponding to the maximum in turbidity, the R_G/R_H ratio started to decrease. A plausible explanation for this change in R_G/R_H ratio is that the aggregates changed structure from dense, hard spheres towards a gel, as has been described for similar systems before.⁴⁰ This explanation is in accordance with the observation that R_H , as determined by DLS, remained at a plateau upon restabilization of the suspension by addition of an excess of anionic starch (see Figure 3). It is also in line with the fact that the turbidity decreased on addition of starch beyond the 1:1 charge ratio of starch to SP+ (Figure 3). The turbidity measurements record the overall density of the aggregates and since they are in a gel-like state the intensity is reduced.

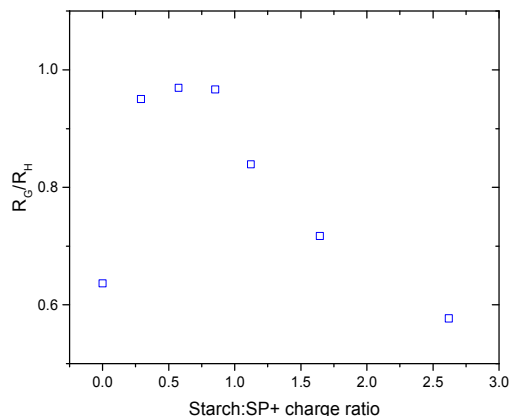


Fig. 4 Ratio of radius of gyration, R_G , to radius of hydration, R_H , vs. starch to particle charge ratio. Note that R_G for the primary particles was obtained from SAXS.

Internal structure of the aggregates

While the R_G/R_H ratios provide valuable information on the macroscopic structure of the aggregates a small angle X-ray scattering (SAXS) investigation was performed to study the internal structure, i.e. the microscopic structure, of the formed aggregates. Scattering data were collected from samples of SP+ particles at 0.1 wt%, from the anionic starch at 3 wt% and from the combination of SP+ particles and the starch at various charge ratios. Two types of starch were used, a regular potato starch composed of 20 wt% amylose and 80 wt% amylopectin and a refined potato starch composed entirely of amylopectin. The latter is an example of a “waxy” starch.

The unified equation has been used to model the scattered intensity.⁴¹ This is an approximated term that describes a complex morphology over a wide range of q in term of structural levels. A structural level in scattering is described by Guinier's law and a structurally limited power law, which on a log-log plot is reflected by a knee and a linear region.

Intensity is modelled using the formula:

$$I(q) = \sum_{i=1}^n G_i \exp\left(\frac{-q^2 R_{G_i}^2}{3}\right) + B_i \exp\left(\frac{-q^2 R_{G_{(i+1)}}}{3}\right) \times \left[\frac{(\text{erf}(qR_{G_i}/\sqrt{6}))}{q}\right]^{3P_i} \quad (1)$$

where n is the number of structural levels, $i=1$ refers to the largest size structure, and $(i+1)$ to the structure of the sub-particle. G is the Guinier prefactor and B is a prefactor specific to this type of power-law scattering. B is defined according to the regime in which the exponent P falls. Generally, for surface fractals $4 > P > 3$, for mass fractals $P < 3$ and for diffuse interfaces $P > 4$.

The q range used in this study, $0.006\text{--}0.4 \text{ \AA}^{-1}$, gives information in a size range matching the primary particles. Log-log plots of the scattering intensity $I(q)$ as a function of the scattering wave vector q for the particles, as well as for the starches, in solution are shown in Figure 5. For both systems, the scattering profile was composed of a single structure level where a Guinier regime at low q value, followed by a power law at high q value, was observed. The data obtained from the

fitting are reported in Table 1. The radius of gyration (R_G) of the SP+ particles was found to be 14 nm. The value of $P = 3.8$ showed that the particle presents a rough fractal surface. This can be explained by the core-shell structure of the SP+ particles where the polymeric stabilizer acts like polymer brushes on the surface.⁴² The two starches had the same scattering profile. The fit to equation (1) yields $R_G = 7 \text{ nm}$ and $P = 2.2$. This indicates that the scattering data for the regular starch was dominated by the amylopectin fraction. The size of 7 nm for the amylopectin is in good agreement with literature values for fractionated amylopectin.⁴³ The value of P is also in line with the value of the fractal dimension of amylopectin rich starch which has been found to lie between $P = 2.5$ (analogous to non-swollen cross-linked cluster) and $P = 2$ (fully swollen cluster).⁴⁴

The structure of the aggregates formed from combinations of starch and SP+ particles were characterized by SAXS within the charge ratio interval 0.19:1 to 3.8:1.

SAXS data, plotted in a log-log diagram of $I(q)$ vs q , are shown in Figure 6. The data were fitted to the unified function (eq. 1). It contains two structure levels ($n=2$), in which four distinguishable features are observed according to their $I(q)$ and q position. At lowest q , a plateau of $I(q)$ value is found and the R_{G1} parameter could be determined. In the scaling regime, the slope of the power law decay $P1$ is observed, which gives the fractal dimension of the aggregates. It follows another plateau of $I(q)$ from where we can determine R_{G2} . At high q value, another power law decay is observed which gives the value of $P2$. These observable structure levels are modelled with an 8 parameters function: $G1, G2, B1, B2, R_{G1}, R_{G2}, P1, P2$. The reported error values were taken from the statistical errors in the experimental data. The values are shown in table 1.

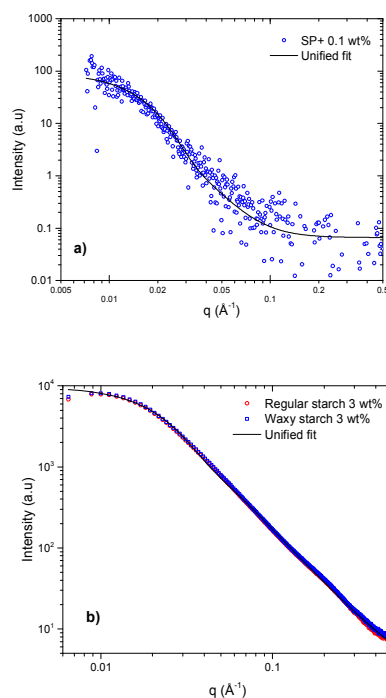


Fig. 5 Log-log plot of SAXS data from SP+ (a) and from regular and waxy starch (b).

Table 1 R_G and P data for SP+, starch and the SP+ and starch mixture from SAXS. (*) Fitted from a single parameter model (R_G , P). As we hypothesize in the double parameter system that R_{G2} and P belong to the starch contribution they are placed in the corresponding column for the sake of clarity.

Sample	Ratio	R_{G1} (Å)	P1	R_{G2} (Å)	P2
SP+	-	140 ± 1	3.8	-	-
Regular starch	-	-	-	70 ± 7 (*)	2.2 (*)
Waxy starch	-	-	-	70 ± 7 (*)	2.2 (*)
Starch : SP+ charge ratio	0.19:1	207 ± 20	4.0	60 ± 1	1.6
Starch : SP+ charge ratio	0.38:1	219 ± 22	3.8	62 ± 2	2.4
Starch : SP+ charge ratio	0.75:1	233 ± 3	3.3	63 ± 2	2.3
Starch : SP+ charge ratio	1.1:1	238 ± 15	3.9	65 ± 2	2.2
Starch : SP+ charge ratio	1.9:1	235 ± 3	3.2	63 ± 1	2.2
Starch : SP+ charge ratio	3.75:1	230 ± 4	2.6	63 ± 10	2.3

The first structure level corresponds to the SP+ particles with adsorbed starch. The size of the aggregate is increasing with increasing starch addition. This means that more and more starch is adsorbed on the surface of the particle, which reaches a maximum size at the starch addition that corresponds to 1:1 in charge ratio. Above this ratio, a slight decrease of R_{G1} followed by a plateau can be observed with increasing starch concentration. This is reasonable because when charge neutralization is reached, the driving force for the adsorption is diminished.

The value of the slope P1 for this level is between $2.6 < P1 < 4$, which shows that the aggregate still has a rough fractal surface covered by starch. However, an overall decreasing trend can be found. One may speculate that this change is caused by a surface densification by closer packing of the starch coils due to minor starch adsorption above the neutralization point. It is likely that this also contributes to the restabilization of the system.

The second structure level corresponds to a branched system with a fractal dimension value P2 between 2 and 3 and a R_{G2} of 6-7 nm. This value is well in line with the value measured for the starch and tends to show that the conformation of the polyelectrolyte is preserved in the presence of the oppositely charge particles. However, it is difficult to confirm that this conformation is derived solely from adsorbed starch, since starch remaining in solution can also contribute.

The SAXS study shows that more and more starch is adsorbed onto the primary SP+ particles up to charge neutralization. This means that the starch is penetrating into the aggregates, not only adsorbing on the outer surface of the aggregates. Further starch additions do not significantly affect the size of R_{G1} , i.e. the starch covered SP+ particles remain intact even though the overall aggregate is now carrying a net anionic charge. As is seen from the turbidity measurement and the changes in R_G/R_H ratio, the overall aggregate size and structure are affected when an excess of starch, in terms of charge ratio, is added to the SP+ particles. This is probably due to additional adsorption of starch on the more accessible,

outer surface of the aggregates, giving rise to the anionic charge that induces repulsion between the aggregates, which give a gel-like structure and a decrease in size. The fact that the size of the starch covered primary particles (R_{G1}) is constant even though the overall aggregates are overcharged may contribute to the stabilization of the aggregates. The aggregates remain stable after weeks of storage.

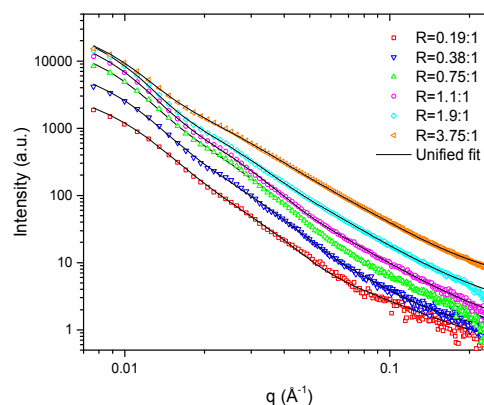


Fig. 6 Log-log plot of SAXS data for combination of starch and SP+ at different charge ratios (R) indicated in the figure. Lines are unified fits to the data.

Adsorption behaviour of amylose and amylopectin during aggregation

As described earlier, starch consists of two types of macromolecules with very different molecular weight, amylose and amylopectin. Size exclusion chromatography, SEC, was employed in order to investigate the possibility of preferential adsorption of one of these components during the aggregation process. A combination of refractive index, RI, and multiple angle light scattering detectors were used, allowing determination of the absolute molecular weight and the molecular weight distribution.

In Figure 7 the RI chromatograms for regular and waxy starch are shown. The regular starch had a bimodal size distribution. The lower molecular weight peak (the peak to the right) is due to amylose chains, and the high molecular weight peak (the peak to the left) is due to amylopectin. The waxy starch only

shows the amylopectin peak. The small amount of low molecular weight compounds in the waxy starch is probably due to depolymerization during the oxidation process. The RI response for the regular starch is in accordance with previous studies, where SEC was used for determining the molecular weight distribution of starch.⁴⁵

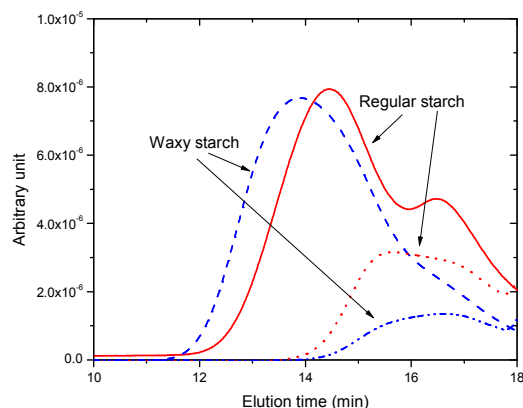


Fig. 7 RI chromatograms for regular and waxy starch (solid lines) and for the starch remaining in solution after aggregation with positively charged particles, SP+, using a starch to particle charge ratio of 1:1 (dashed lines).

In order to determine the composition of the starch that had participated in the aggregation process, varying amounts of a 3 wt% starch solution (regular or waxy) were added to a 0.1 wt% particle suspension. The experiments were designed so that the charge ratio that gave maximum turbidity (1:1, see Figure 3) was covered. After each addition the mixture was centrifuged and the supernatant filtered before analysis by SEC. As reference, a starch solution was centrifuged, filtered and analysed in the SEC system. With this method the starch remaining in solution, i.e. the starch that is not taking part in the aggregation with the cationic particles, is determined.

The SEC analyses of the samples revealed an interesting pattern. For the starch-particle combinations where charged neutralization was not yet obtained, i.e. at low starch to particle ratio, the RI chromatogram showed that the fraction corresponding to higher molecular weights, i.e. the amylopectin, had disappeared. For the regular starch, which contains a mixture of amylose and amylopectin, it was found that a significant part of the lower molecular weight fraction of the starch, i.e. the amylose, remained in solution even though the starch was in deficit. Thus, it seems that only the amylopectin fraction of the regular starch took part in the aggregation with the oppositely charged particles. The fact that the amylose fraction did not much contribute, at equilibrium, to the aggregation is interesting. It could be due to lower charge density of amylose than of amylopectin. However, that is unlikely because both amylose and amylopectin consist of anhydroglucose rings and their tendency to generate carboxylate groups during the NaClO oxidation should be approximately the same.^{45, 46} Initially the amylose chains might adsorb on the particle surface before the amylopectin chains due to faster diffusion of the shorter amylose⁴⁷ and the higher molecular weight amylopectin may

subsequently gradually replace the amylose on the surface. However, such a competitive adsorption between the two starch components,⁴⁸ could not be observed in this study since the measurements were made after equilibration.

Figure 7 also shows that for the waxy starch, which contains only amylopectin, only the lower molecular weight fraction, which may originate from depolymerization during the oxidation stage, see above, is found in solution after the aggregation.

The observation that it is the amylopectin fraction of the starch that is responsible for the aggregation is interesting and can help explaining why the formed aggregates are stable despite their low charge density. There is not much electrostatic stabilization left but the highly branched and negatively charged amylopectin molecules that cover the positively charged particles are likely to give good steric stabilization. This is a proper example of so-called electrosteric repulsion.⁴⁷

Mechanism of aggregation

Possible mechanisms for polyelectrolyte-induced aggregation of colloidal particles of opposite charge are extensively discussed in the literature and two different mechanisms are in focus. Bridging flocculation can occur when one part of the polymer chain is adsorbed on one particle surface while the rest of the polymer chain remains in the bulk from where it may eventually adsorb onto another particle surface, thereby forming a bridge between the particles.⁴⁹ This aggregation mechanism requires concentrated suspensions and high molecular weight polymers.³⁷ The other important aggregation mechanism that is discussed in the literature is patchwise flocculation.^{4, 5, 7, 30, 50-53} A charged polymer chain adsorbs onto the particle surface due to electrostatic attraction. This leads to a local charge reversal on the part of the particle surface that has been covered; thus, the particle surface now contains patches of opposite charge. This may lead to electrostatic attraction between covered patches on one particle and uncovered patches on another particle. Regular starch, which is used in the present study, can be regarded as a mixture of two rather dissimilar polyelectrolytes, the linear and low molecular weight amylose and the branched and high molecular weight amylopectin. The SEC results discussed above showed that it is mainly the amylopectin fraction that participates in the aggregation process. Figure 8 is an attempt to visualize the aggregation.

The turbidity data indicate that aggregation starts already at a low ratio between the anionic starch and the positively charged particles. At this stage the primary particles, as well as the aggregates formed, will carry a positive net charge. As demonstrated by the SEC experiments, amylopectin molecules have started to adsorb on the positively charged particles and it is this adsorption that is responsible for the aggregation. As discussed above, there are two main aggregation mechanisms, bridging flocculation and patch-wise flocculation.

Since the particle concentration used in the present series of experiments is low, 0.1 wt%, and the molecular weight of the PE is also relatively low, bridging flocculation is less likely. It is therefore probable that the aggregation is due to patch-wise flocculation. This means that sites on the particles that

are covered with adsorbed amylopectin will undergo charge reversal and become negative. Such sites will be attracted by the positively charged sites of naked surface of other particles. Aggregation will take place, as is reflected by the increase in size of the aggregates as measured by DLS and by the lowering of the ζ potential indicating gradual neutralization of the complexes. In addition, the SEC results show that, even though starch is in deficit, a substantial amount of the amylose fraction does not participate in the aggregation but remains in solution.

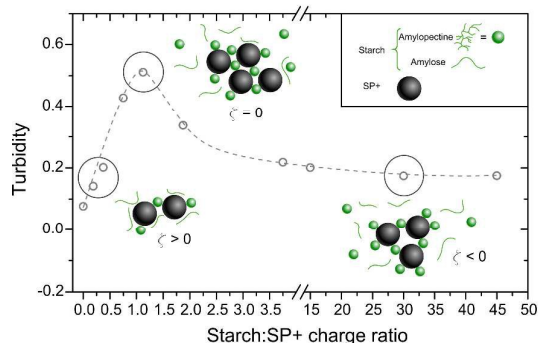


Fig. 8 Tentative mechanism for aggregation of regular starch, which is negatively charged and consists of a mixture of amylose and amylopectin, and positively charged particles.

This is well reflected by the data from the SAXS fitting that indicates that during the aggregate formation two distinct regimes can be observed, one corresponding to a coiled polymer, i.e. the amylopectin (R_{G2}) and one to a larger structure, i.e. the aggregates formed by SP+ and starch (R_{G1}). The latter structure keeps increasing, as expected for particles onto which increasing amount of polymer has adsorbed. Furthermore, a densification of the aggregates is observed.

At the point of charge reversal, the particle surface is covered by coiled starch chains to the extent that the cationic charges are fully neutralized and the particle suspension is then totally destabilized. The coverage is also reflected by the SAXS data, since the R_{G1} is reaching a plateau around the point of charge reversal.

At starch concentrations above the 1:1 charge ratio the turbidity starts to decrease. This is in accordance with the drop in the R_G/R_H ratio. At high starch concentrations this ratio decreases, indicating a change from a hard sphere to a gel structure. This transformation gives rise to a less dense structure, as seen by a decrease in turbidity. From the SAXS data it was found that the structure and size of the starch covered primary particles remain more or less unchanged. The SEC data show that amylopectin is still adsorbing on the particle surfaces even though the neutralization point is exceeded. This is confirmed by the ζ potential data. At a starch to particle charge ratio above 1, the ζ potential is negative and levels out at -8 mV. Thus, the aggregates have undergone charge reversal and do now carry a negative net charge. A value of -8 mV is small, however, and will not lead to strong electrostatic stabilization. Yet, the system exhibits a very high colloidal stability. One may therefore assume that the

adsorption of amylopectin, owing to its branched nature, gives rise to effective electrosteric stabilization.

Conclusion

The aggregation of cationic nanoparticles and anionic starch, composed of 20 wt% amylose and 80 wt% amylopectin, was monitored by turbidity, DLS, SLS, SAXS and SEC. From the turbidity studies the aggregation behaviour was determined. A small addition of the starch induced aggregation of the cationic particles with the oppositely charged polymer, until a 1:1 charge ratio was reached. At higher charge ratio, the aggregates regained stability. This phenomenon has been studied for many systems before, but the analytical techniques used here reveal the structure and composition of the formed aggregates.

In this study it was demonstrated that the charge of the aggregated system was only partially reversed when starch was added in excess. Even at high starch concentration the aggregates were stable in solution, as a result of the starch adsorbing on the particle surfaces. The addition order did not change the aggregation behaviour.

The SEC study showed that it is mostly the branched amylopectin component of the starch that gives rise to the aggregation with the cationic particles. The low molecular weight amylose remains in solution. This indicates a change of stabilization mechanism from electrostatic (for the primary particles) to electrosteric. This is confirmed with SAXS where a densification of the starch layer within the aggregates was seen after charge neutralization leading to restabilization of the system. Furthermore the SAXS measurements showed that the amylopectin conformation was partly preserved. This confirms a patchwise aggregation mechanism where the starch chains locally change the surface charge from cationic to anionic. The negatively charged sites will be attracted by the positively charged sites of naked surface of other particles, leading to aggregation.

The aggregation behaviour and the selective adsorption of the highly branched amylopectin when cationic nanoparticles and anionic starch are combined can give insight and knowledge relevant for the practical applications of these systems.

Acknowledgement

Financial support from the Swedish Research Council is gratefully acknowledged.

The opportunity to go to MAX IV Laboratory for SAXS beam time is gratefully acknowledged.

SuMo Biomaterials is gratefully acknowledged for economic and scientific support.

References

1. M. Borkovec and G. Papastavrou, *Current Opinion in Colloid and Interface Science*, 2008, **13**, 429-437.
2. A. Fuchs and E. Killmann, *Colloid and Polymer Science*, 2001, **279**, 53-60.

3. J. Gregory, *Journal of Colloid And Interface Science*, 1976, **55**, 35-44.
4. F. Mabire, R. Audebert and C. Quivoron, *Journal of Colloid And Interface Science*, 1984, **97**, 120-136.
5. J. Zhang, C. Huguenard, C. Scarnecchia, R. Menghetti and J. Buffle, *Colloids and Surfaces A: Physicochemical and Engineering Aspects*, 1999, **151**, 49-63.
6. G. Carlsson and J. Van Stam, *Nordic Pulp and Paper Research Journal*, 2005, **20**, 192-199.
7. J. Gregory, *Journal of Colloid and Interface Science*, 1973, **42**, 448-456.
8. W. L. Yu, F. Bouyer and M. Borkovec, *Journal of Colloid and Interface Science*, 2001, **241**, 392-399.
9. A. A. Meier-Koll, C. C. Fleck and H. H. Von Grünberg, *Journal of Physics Condensed Matter*, 2004, **16**, 6041-6052.
10. S. Rosenfeldt, A. Wittemann, M. Ballauff, E. Breininger, J. Bolze and N. Dingenouts, *Physical Review E - Statistical, Nonlinear, and Soft Matter Physics*, 2004, **70**, 061403-061401-061403-061410.
11. K. Holmberg, B. Jönsson, B. Kronberg and B. Lindman, *Surfactants and Polymers in Aqueous Solution, 2nd ed.*, Wiley, Chichester, 2003.
12. E. Seyrek, J. Hierrezuelo, A. Sadeghpour, I. Szilagyi and M. Borkovec, *Physical Chemistry Chemical Physics*, 2011, **13**, 12716-12719.
13. M. Borkovec, I. Szilagyi, I. Popa, M. Finessi, P. Sinha, P. Maroni and G. Papastavrou, *Advances in Colloid and Interface Science*, 2012, **179-182**, 85-98.
14. P. M. Claesson, A. Dedinaite and O. J. Rojas, *Advances in Colloid and Interface Science*, 2003, **104**, 53-74.
15. Y. K. Leong, P. J. Scales, T. W. Healy and D. V. Boger, *Colloids and Surfaces A: Physicochemical and Engineering Aspects*, 1995, **95**, 43-52.
16. P. M. Claesson, E. Poptoshev, E. Blomberg and A. Dedinaite, *Advances in Colloid and Interface Science*, 2005, **114-115**, 173-187.
17. T. Nypelö, M. Österberg, X. Zu and J. Laine, *Colloids and Surfaces A: Physicochemical and Engineering Aspects*, 2011, **392**, 313-321.
18. D. Solberg and L. Wågberg, *Colloids and Surfaces A: Physicochemical and Engineering Aspects*, 2003, **219**, 161-172.
19. E. Gustafsson, P. A. Larsson and L. Wågberg, *Colloids and Surfaces A: Physicochemical and Engineering Aspects*, 2012, **414**, 415-421.
20. R. Carceller and A. Juppo, *Paperi ja Puu/Paper and Timber*, 2004, **86**, 161-163.
21. F. Iselau, P. Restorp, M. Andersson and R. Bordes, *Colloids and Surfaces A: Physicochemical and Engineering Aspects*, 2015, **483**, 264-270.
22. W. Brown, *Dynamic light scattering: the method and some applications.*, Clarendon Press, Oxford, 1993.
23. K. Schätzel and J. Merz, *J. Chem. Phys.*, 1984, **81**, 2482-2488.
24. K. Böckenhoff and W. R. Fischer, *Fresenius' Journal of Analytical Chemistry*, 2001, **371**, 670-674.
25. R. Wäsche, M. Naito and V. A. Hackley, *Powder Technology*, 2002, **123**, 275-281.
26. J. Ilavsky, *J. Appl. Crystallogr.*, 2012, **45**, 324-328.
27. S. Chakraborty, B. Sahoo, I. Teraoka and R. A. Gross, *Carbohydrate Polymers*, 2005, **60**, 475-481.
28. J. J. M. Swinkels, *Starch - Stärke*, 1985, **37**, 1-5.
29. D. Kuakpetoon and Y. J. Wang, *Starch - Stärke*, 2001, **53**, 211-218.
30. G. Gillies, W. Lin and M. Borkovec, *Journal of Physical Chemistry B*, 2007, **111**, 8626-8633.
31. E. S. Dragan and S. Schwarz, *Journal of Polymer Science, Part A: Polymer Chemistry*, 2004, **42**, 5244-5252.
32. C. Ankerfors, S. Ondaral, L. Wågberg and L. Ödberg, *J. Colloid Interface Sci.*, 2010, **351**, 88-95.
33. N. P. Birch and J. D. Schiffman, *Langmuir*, 2014, **30**, 3441-3447.
34. L. Štajner, J. Požar and D. Kovačević, *Colloids and Surfaces A: Physicochemical and Engineering Aspects*, 2015, **483**, 171-180.
35. V. K. La Mer, R. H. Smellie Jr and P. K. Lee, *Journal of Colloid Science*, 1957, **12**, 230-239.
36. L. F. Albright and Knovel, *Albright's Chemical Engineering Handbook*, CRC Press, Boca Raton, 2009.
37. H. W. Walker and S. B. Grant, *Colloids and Surfaces A: Physicochemical and Engineering Aspects*, 1996, **119**, 229-239.
38. A. Sadeghpour, E. Seyrek, I. Szilazgyi, J. Hierrezuelo and M. Borkovec, *Langmuir*, 2011, **27**, 9270-9276.
39. B. Hirzinger, M. Helmstedt and J. Stejskal, *Polymer*, 2000, **41**, 2883-2891.
40. D. Kunz, A. Thurn and W. Burchard, *Colloid. Polym. Sci.*, 1983, **261**, 635-644.
41. G. Beaucage, *Journal of Applied Crystallography*, 1995, **28**, 717-728.
42. X. Chen, J. Zhang, Z. Yi, Q. Wang, X. Li, F. Bian, J. Wang and Y. Men, *Journal of Coatings Technology Research*, 2011, **8**, 489-496.
43. D. Sarazin, J. H. François, C. Verwaerde and G. Flèche, *Journal of Applied Polymer Science*, 1992, **46**, 715-724.
44. P. Roger and P. Colonna, in *Light Scattering and Photon Correlation Spectroscopy*, eds. E. R. Pike and J. B. Abbiss, Springer Netherlands, 1997, vol. 40, ch. 18, pp. 225-229.
45. D. Kuakpetoon and Y. J. Wang, *Carbohydrate Research*, 2006, **341**, 1896-1915.
46. Y. J. Wang and L. Wang, *Carbohydrate Polymers*, 2003, **52**, 207-217.
47. B. Kronberg, K. Holmberg and B. Lindman, *Surface Chemistry of Surfactants and Polymers*, Wiley, Chichester, 2014.
48. Z. Fu and M. M. Santore, *Macromolecules*, 1998, **31**, 7014-7022.

Journal Name

ARTICLE

49. T. W. Healy and V. K. La Mer, *Journal of Colloid Science*, 1964, **19**, 323-332.
50. Y. Shin, J. E. Roberts and M. M. Santore, *Journal of Colloid and Interface Science*, 2002, **247**, 220-230.
51. K. Furusawa, M. Kanesaka and S. Yamashita, *Journal of Colloid And Interface Science*, 1984, **99**, 341-348.
52. S. Schwarz, H. M. Buchhammer, K. Lunchwitz and H. J. Jacobasch, *Colloids and Surfaces A: Physicochemical and Engineering Aspects*, 1998, **140**, 377-384.
53. Y. Chen, S. Liu and G. Wang, *Chemical Engineering Journal*, 2007, **133**, 325-333.

